
# Politecnico di Milano

# Orbital Mechanics
# Academic Year 2023/2024

# Group ID: 2338


| | Matriculation number | Person code |
|---|---|---|
| **Biraghi Giacomo** | **243039** | **10725818** |
| **Cattaneo Marco** | **250002** | **10711761** |
| **Frassinella Luca** | **244643** | **10795356** |
| **Scudier Gianluca** | **242253** | **10697668** |

# Index


**1.** Interplanetary mission
- **1.1.**Introduction
- **1.2.**Design process
  - **1.2.1.** Constraints
  - **1.2.2.** Assumptions
  - **1.2.3.** Preliminary analysis
- **1.3.**Solution processes
  - **1.3.1.** Grid Search optimization
  - **1.3.2.** Genetic Algorithm optimization
- **1.4.**Results
  - **1.4.1.** Final results
  - **1.4.2.** Final mission
  - **1.4.3.** Final comments

**2.** Planetary Explorer Mission
- **2.1.**Introduction and nominal orbit definition
- **2.2.**Ground tracks
- **2.3.**Propagation with J2 and SRP
- **2.4.**History of the Keplerian elements
- **2.5.**Evolution of the orbit
- **2.6.**Filters
- **2.7.**Comparison with real data

# 1. INTERPLANETARY MISSION

## 1.1 INTRODUCTION

The PoliMi Space Agency is carrying out a feasibility study for an Interplanetary Explorer Mission visiting three celestial bodies in the solar system: Mercury, Venus and Asteroid 2001 TW229.
The focus of this study is to analyse the possible transfer options from Mercury to the Asteroid, performing a powered gravity assist around Venus and determining the optimal departure, fly-by and arrival dates to minimize the total cost (in terms of $\Delta v$ ) of the mission.

## 1.2 DESIGN PROCESS

### 1.2.1 Constraints

The mission must satisfy the following constraints:

- Earliest date of departure: $01/01/2028$
- Latest date of arrival: $01/01/2058$
- Minimum altitude of the powered gravity assist hyperbola: $450\ km$

### 1.2.2 Assumptions

For this study, the patched conics method has been used, under the following assumptions:

- The starting orbit is the same of the departure planet, in the heliocentric frame
- The final orbit is the same of the arrival body, in the heliocentric frame
- In the planetocentric frame, the sphere of influence of the planet (SOI) is assumed infinite
- In the heliocentric frame, the sphere of influence of the planet (SOI) is assumed negligible
- The powered gravity assist manoeuvre is assumed instantaneous in the heliocentric frame, while it has a finite time in the planetocentric frame
- All manoeuvres in the heliocentric frame are considered instantaneous
- Solar Radiation Perturbations have been ignored

### 1.2.3 Preliminary analysis

A preliminary analysis has been conducted to reduce the windows for the time of flights of the two lambert arcs, from Mercury to Venus and from Venus to Asteroid 2001 TW229.

For this purpose, the cost plots for both departure and arrival manoeuvres have been computed and analysed, as can be seen in figure 1 and 2. Every manoeuvre with a cost higher than 15 km/s has not been plotted, to have a clean representation of only the combinations of dates that resulted in an acceptable cost of departure and arrival.
The plots revealed that the first time of flight can be taken, in first approximation, between 50 and 200 days, while the second one can be between 80 and 400 days, since for longer or shorter times of flight the cost of the impulsive manoeuvres would be too high.
For the Grid Search Optimization other considerations, based on the synodic periods, have been done to decide the frequency of departures for the preliminary analysis and will be discussed later on in the report.

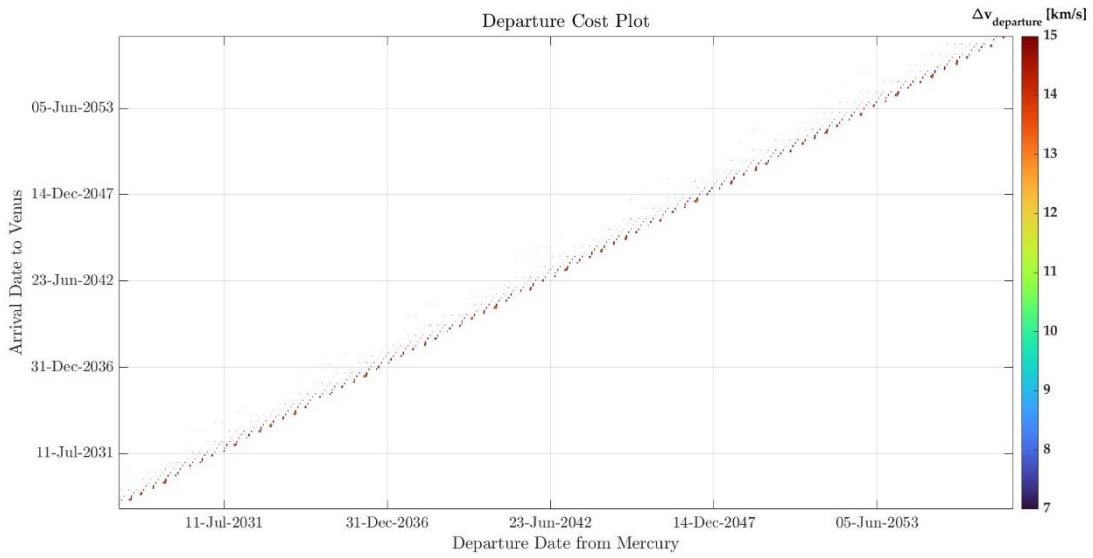


*Figure 1 - Cost Plot of the departures from Mercury*

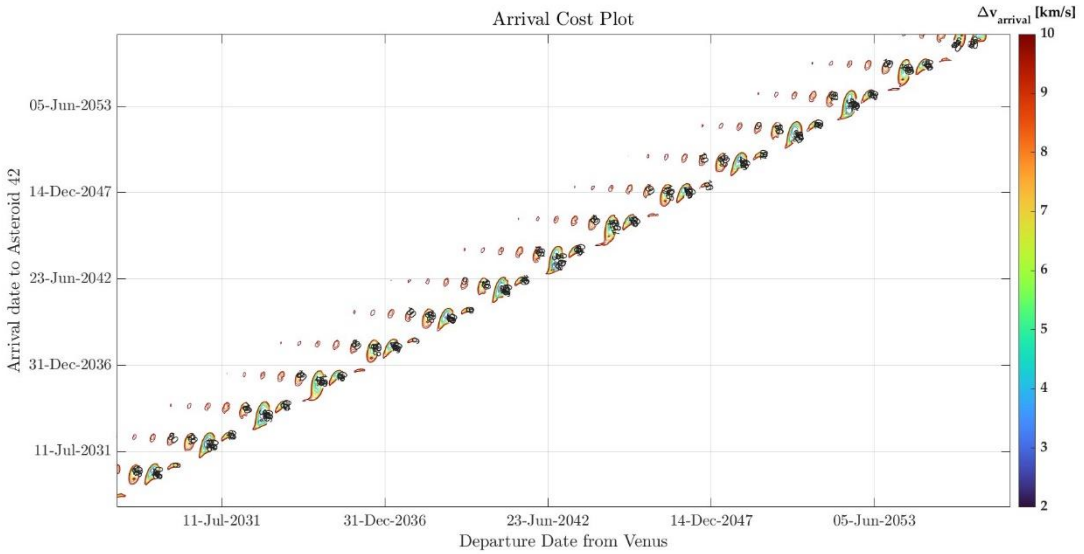


*Figure 2 - Cost plot of arrivals to Asteroid 2001 TW229*

At the end of the preliminary estimations, the following time windows have been chosen to begin the optimization processes:

| **Departure dates** | | **First Interplanetary leg** | | **Second Interplanetary leg** | |
|---|---|---|---|---|---|
| Earliest | Latest | Min. Duration [days] | Max. Duration [days] | Min. Duration [days] | Max. Duration [days] |
| 01/01/2028 | 01/01/2058 | 50 | 200 | 80 | 400 |

*Table 1 - Preliminary time windows*

## 1.3 SOLUTION PROCESSES

Since the departure, fly-by and arrival bodies are fixed, the cost of the mission is dependent only on the following three variables:

- The date of departure (`departure time`)
- The duration of the first interplanetary leg (`TOF1`)
- The duration of the second interplanetary leg (`TOF2`)

To optimize the mission two different optimization methods have been implemented: a Grid Search optimization to compute a minimum starting from a coarse discretization and a Genetic Algorithm optimization to find a more precise minimum starting from the results obtained from the first analysis.

### 1.3.1 Grid Search optimization

The implemented grid search method uses two functions (`interplanetary_opt` and `refineGrid`) and works on four consecutive steps: from an initial coarse grid with departures every 100 days to a final precision of one minute in the dates for the last step.

The first function performs the optimization algorithm and finds the minimum cost and the corresponding dates of departure, fly-by and arrival for each of the five steps.
The second function, instead, takes the outputs of the algorithm to refine the grid for the next step, updating the precision to “day”, “hour”, and at last “minute”.

The grid search optimization is based on the following process:

```
1) Define initial (coarse) grid
2) 1st step optimization:
   for each departure time
         for each TOF1
               for each TOF2
                     compute and store DV(dep, tof1, tof2)
               end
         end
   end
   Find minimum DV (that satisfies the constraints) and save depDate,
   flybyDate, arrDate
3) Refine grid based on the found optimal dates
4) 2nd step optimization
5) Refine grid based on the found optimal dates
6) 3rd step optimization
7) Refine grid based on the found optimal dates
8) 4th step optimization
9) Refine grid based on the found optimal dates
10) 5th step optimization
```

A departure every 100 days has been chosen to have a value close to the synodic period of Mercury with respect to Venus:

$$T_{syn} = 144.57\ days$$

### 1.3.2 Genetic Algorithm optimization

The genetic algorithm is an optimization process that allows to find the minimum of a fitness function constrained by upper and lower boundary conditions. To solve this problem, the `ga.m` function of Matlab has been used, the fitness function is the one of the total interplanetary mission and the algorithm takes as inputs the earliest date of departure, the latest date of arrival and the time duration of the two interplanetary legs that were computed by the Grid Search process, as can be seen in Table 2.

| | |
|---|---|
| Earliest date of Departure | $01/10/2051 \;\; 00:00:00$ |
| Latest date of Arrival | $31/10/2051 \;\; 00:00:00$ |
| First leg maximum Time of Flight | $200\ days$ |
| Second leg maximum Time of Flight | $200\ days$ |

*Table 2 - Time windows for the Genetic Algorithm*

This process has been used to find a more precise result in the proximity of the one computed in the previous analysis, with a precision of seconds in the dates of departure, fly-by and arrival.

The two fundamental parameters for the `ga.m` function are the population size and the maximum total number of generations: they both must be high enough to allow the convergence of the algorithm with a good enough precision, but increasing the parameters too much would result in a higher computational cost. For this reason, a good compromise was found to be:

- Population size: 1000
- Maximum number of generations: 500

Since the Genetic Algorithm does not give the same solution every time, a decision was made to run the code ten times and the mission that provided the overall minimum $\Delta v$ was chosen.

## 1.4 RESULTS

### 1.4.1 Final results

Table 3 shows the results of the two different optimization processes.
As can be seen, the Genetic Algorithm found a smaller minimum in terms of $\Delta v$ and was therefore chosen to characterize the optimal Interplanetary Mission.

| **Process** | **Departure [mjd2000]** | **Fly-by [mjd2000]** | **Arrival [mjd2000]** | $\Delta t_{tot}$ **[days]** | $\Delta v_{tot}$ **[km/s]** |
|---|---|---|---|---|---|
| **Grid Search** | 18926.57 | 19111.71 | 19277.22 | 350.65 | **19.1176** |
| **Genetic Algorithm** | 18927.44 | 19113.92 | 19283.16 | 355.72 | **18.9349** |

*Table 3 - Results obtained with the Grid Search and Genetic algorithms*

### 1.4.2 Final mission

In table 4 are reported the chosen dates for the final optimal mission:

| | |
|---|---|
| **Departure Date** | 27/10/2051 22:36:00 |
| **Fly-by Date** | 01/05/2052 10:09:29 |
| **Arrival Date** | 17/10/2052 15:54:22 |

*Table 4 - Departure, Flyby and Arrival dates of the optimal mission*

In table 5 are reported the cost of the single manoeuvres, as well as the total cost of the mission:

| **Manoeuvre** | **Cost [km/s]** |
|---|---|
| Departure | 11.2833 |
| Powered Gravity Assist | $9.7803 \cdot 10^{-5}$ |
| Arrival | 7.6515 |
| **Total Mission** | **18.9349** |

*Table 5 - Cost of the single manoeuvres and total cost of the mission*

In table 6 The orbital elements for the first and second interplanetary trajectories are showcased:

| | **a [km]** | **e [-]** | **i [°]** | **Ω [°]** | **$\omega$ [°]** | **$\theta$ [°]** | |
|---|---|---|---|---|---|---|---|
| **First trajectory** | $1.073 \cdot 10^8$ | 0.3978 | 6.98 | 48.50 | 272.17 | 333.9 | 245.7 |
| **Second trajectory** | $1.492 \cdot 10^8$ | 0.4445 | 2.92 | 90.65 | 191.66 | 284.2 | 160.4 |

*Table 6 - Orbital elements of the first and second transfer leg*

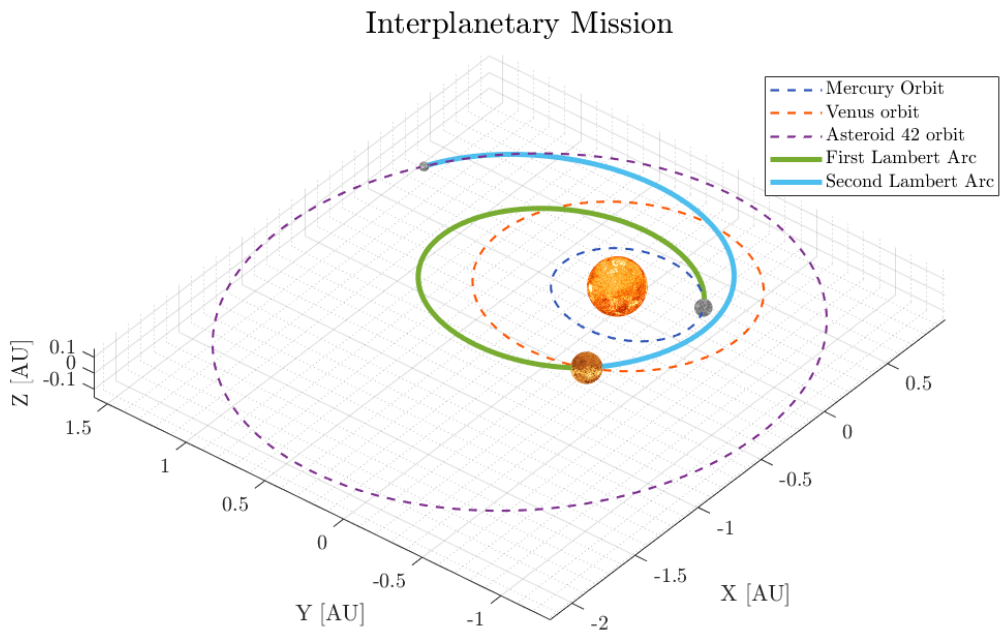


*Figure 3 - Heliocentric plot of the optimal mission's trajectories*

For the fly-by, the incoming and outgoing velocities of the spacecraft in the Heliocentric frame are:

$$V_{sc}^{-} = \begin{Bmatrix} 26.51 \\ -22.36 \\ -4.25 \end{Bmatrix} \text{ [km/s]}; \quad V_{sc}^{+} = \begin{Bmatrix} 29.26 \\ -26.65 \\ -1.48 \end{Bmatrix} \text{ [km/s]}; \quad \Delta v_{flyby} = |V_{sc}^{+} - V_{sc}^{-}| = 5.79 \text{ [km/s]}$$

The ratio between the cost of the impulse given at the pericentre of the hyperbola and the total velocity gain obtained with the fly-by is:

$$\frac{\Delta v_{@pericentre}}{\Delta v_{flyby}} = 1.689 \cdot 10^{-5}$$

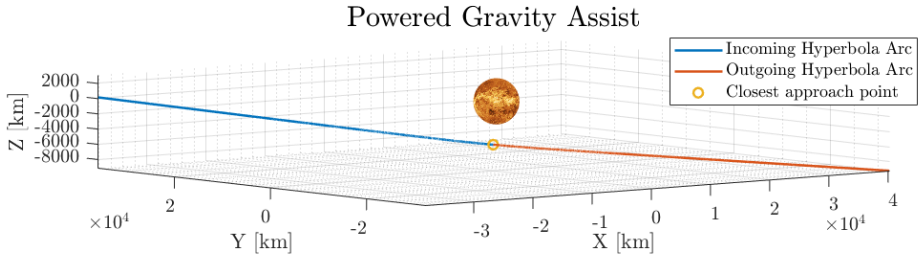


*Figure 4 - Planetocentric plot of the incoming and outgoing hyperbola arcs*

The closest approach to Venus will take place on May 1st 2052 at 10:09:29 at an estimated altitude of:

$$h_{PGA} = 491.789\ km$$

The total time duration of the fly-by, considering a finite sphere of influence of Venus (SOI), is:

$$\Delta t_{flyby} = 23h05m23s$$

### 1.4.3 Final comments

The first manoeuvre is the most expensive one, since Mercury's orbit lies on a different plane. The powered gravity assist, instead, is by far the least expensive manoeuvre, since the turn angle of the two hyperbolic legs is almost identical and this results in a very low impulse at the perigee of the flyby.

In conclusion, the single manoeuvres for departure and arrival are way more expensive than the single optimal values computed in the preliminary analysis, but it must be kept in consideration that the minimum cost of each Lambert arc doesn't correspond to the optimal values for the total mission and a compromise with suboptimal manoeuvres had to be found.

To furthermore lower the cost of the mission, multiple flybys around Venus could be performed, even if this would result in a greater time duration of the mission.

# 2. PLANETARY EXPLORER MISSION

## 2.1 INTRODUCTION AND NOMINAL ORBIT DEFINITION

The planetary explorer mission is considering the launch of a satellite for Earth observation. The team opted for a slightly elliptical and geostationary orbit, with a high inclination to cover the Earth's parts of interest. The data are the following:

| a [km] | e [-] | i [deg] | OM [deg] | om [deg] | f [deg] |
|---|---|---|---|---|---|
| 42161 | 0.0035 | 54.2081 | 0 | 0 | 0 |

The first data, a, is the semi-major axis of the orbit, e is the eccentricity, i is the inclination of the orbit considering the equator as 0 degrees, OM is the right ascension of the ascending node, imposed null as the argument of perigee om and the true anomaly f.

## 2.2 GROUND TRACKS

The team studied the ground track of the orbit evaluating different cases.
Considering the case of the unperturbed ground track, we can track the orbit computing the ascension and the declination knowing the state vector of the satellite along the orbit. From these, we can have the longitude and the latitude in degrees at each time.
The repeating ground track is instead obtained computing the repeating semi-major axis of the orbit knowing the Earth's number of rotations and the satellite's number of revolutions around the Earth in the time of interest. These two assigned parameters (m, k) are both equal to one, so the repeating semi-major axis is equal to the original semi-major axis. We can then obtain the state vector of the repeating ground track using the repeating semi-major axis.

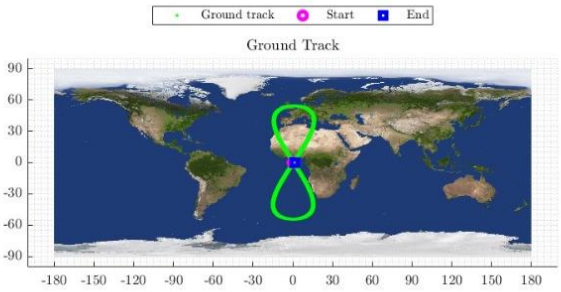


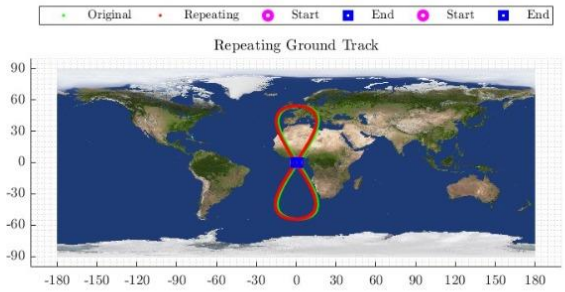


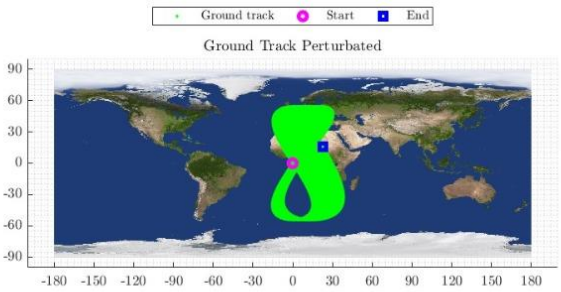


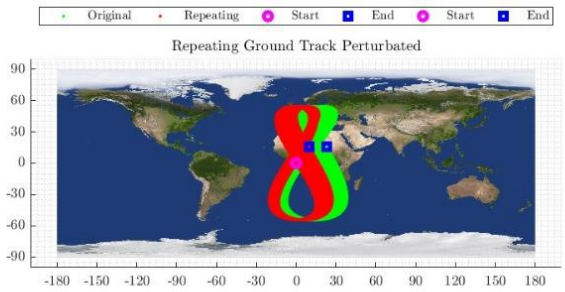

Eventually the perturbed repeated ground track is computed, considering also the J2 gravitational perturbation of the Earth and the solar radiation pressure. The state vector in this case is determined considering also the accelerations of the J2 perturbation:

$$\vec{a}_{J2} = \frac{3}{2}\frac{J2\ \mu_E\ {R_p}^2}{r^4}\left[\frac{x_i}{r}\left(\frac{5z^2}{r^2} - 1\right)\right]$$

and the acceleration of the solar radiation pressure

$$\vec{a}_{SRP} = -p_{sr@1AU}\frac{AU^2}{\|\vec{r}_{sc-Sun}\|}C_r\frac{A_{Sun}}{m}\frac{\vec{r}_{sc-Sun}}{\|\vec{r}_{sc-Sun}\|}$$

The J2 perturbation is a harmonic perturbation caused by the oblateness of the Earth which generates a paucity of the symmetry of the considered celestial body. The solar radiation pressure instead is caused by the electromagnetic radiation expelled by the Sun. That kind of radiation generates a pressure on the body of the spacecraft and perturbs its motion.
We can here observe that the perturbed repeated problem still works even considering the perturbations, we get perturbed paths and disturbed starting and ending point but even now we can work and study the mission.

## 2.3 PROPAGATION WITH J2 AND SRP

The orbit is propagated considering the J2 perturbation and the solar radiation pressure in cartesian coordinates, evaluating the perturbed state vector, and also studying the Keplerian elements, obtained computing the Gauss's planetary equations in tangential, normal, out-of-plane reference frame {t,n,h}. The propagation is obtained integrating numerically using the ode113 Matlab function, having in input the perturbed equation of motion.

## 2.4 HISTORY OF THE KEPLERIAN ELEMENTS

The history of the Keplerian elements of the orbit is studied considering a propagation time of 20 and 200 periods, which is enough to see the effect of the perturbations, since the chosen orbit is almost circular and geostationary, so the perturbations do not have a great effect in the near time.
The semi-major axis "a" oscillates around its nominal value in the order of 10 km in approximately 1 period of the orbit. This oscillation remains stable during all the time considered. The relative error between the cartesian and the gauss propagation stands in the order of $10^{-13}$, but we can observe some low peaks in the error. The error though starts increasing at the end due to the prolonged effect of the perturbations.
The eccentricity "e" increases during all the evaluated time. That is confirmed by the theory, the principal effect of the solar radiation pressure is indeed to increase the eccentricity of the affected orbit. The error regarding the eccentricity is between $10^{-14}$ and $10^{-13}$.
Considering now the inclination "i", we can here observe that we have 2 kinds of oscillations, the first one is in a single period of the orbit in the order of $0{,}05^{\circ}$, while the second one is observable in a long period of time, here 200 periods, and the oscillation is between 54,225° and 54,205°. The two oscillations are combined during the total time of observation. We can also check the cartesian and the gaussian propagation, and we can see that until the 150 periods it stays nearly or below the $10^{-15}$, while going on with the total time it starts increasing.

The Right ascension of the ascending node "Ω" is mainly affected by the gravitational perturbation J2. Indeed, we can observe the Nodal regression, which is a variation of the RAAN over time. It is dependent on the inclination, and having a i < 90° means that the Ω decreases over time, so we have a westward rotation of the orbit. The absolute error between the cartesian and the Gauss propagation is considerable as constant over 75 periods, with the value always in the order of $10^{-15}$, while before that moment it oscillates between $10^{-20}$ and $10^{-15}$.
The argument of pericentre "ω" i also mostly affected by the J2 perturbation, we can see with the graphs the Perigee precession. It is a variation of the argument of pericentre over time and depends on the inclination. Having an inclination less than 63,4° we have an increasing effect over time. The first part of the graph though decreases due to the computation of ω in the gauss propagation, in fact the formula is firstly divided by the eccentricity, which is nearly zero in the first stages of the considered time. The error is almost constant in the order of $10^{-12}$ or $10^{-11}$, but starts increasing after 150 periods.
The true anomaly "f" represents the evolution of the angular position of the satellite on the orbit and increases from 0° up to 360°. The computation considering the cartesian and the Gauss propagation oscillates during the period, having a maximum of $10^{-10}$ in the first part and a minimum of $10^{-16}$.

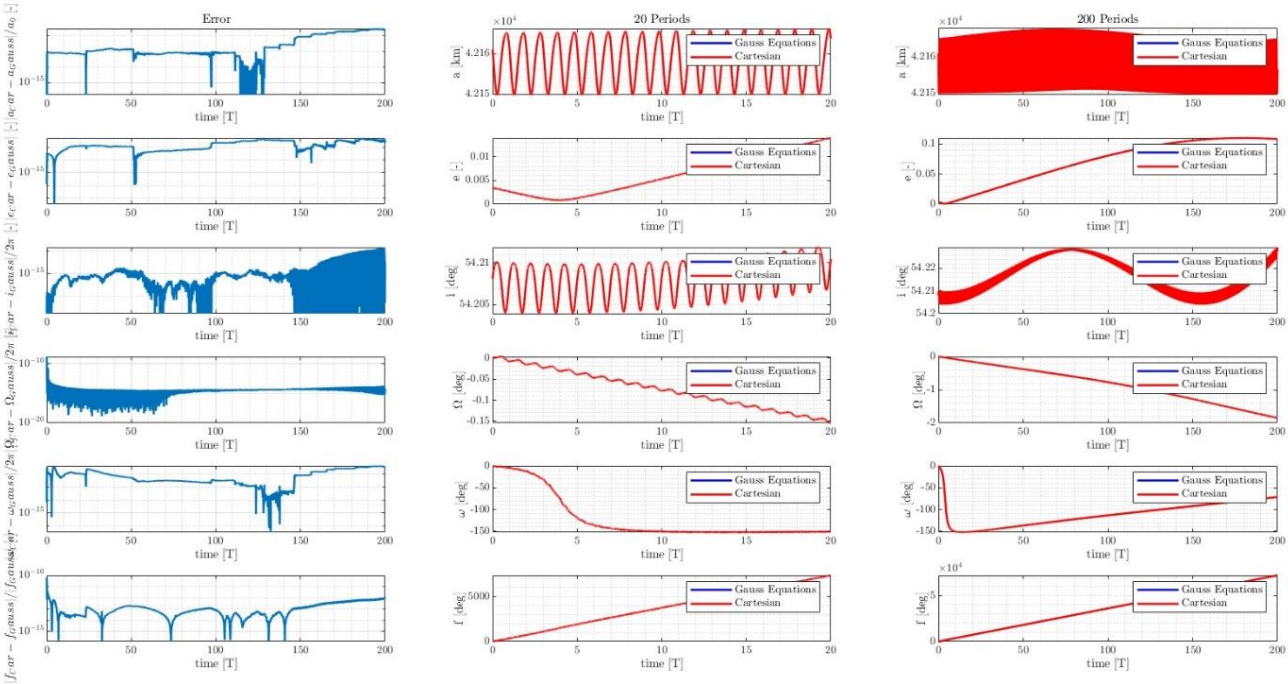


The cartesian propagation consists of the integration of a set of ordinary differential equations on a given time span, which is set as a multiple of the period of the orbit. The ODEs are a the derivate state vector containing velocities and accelerations, after adding to the last ones the perturbed accelerations due to J2 and solar radiation pressure in the {x,y,z} reference frame. The ode113 integrations provides a matrix containing all the state vectors in the time span. After the integration, we get the Keplerian elements from the state vector at each time using the conversation from state vector to Keplerian elements. The computational time, which includes the integration of the equation of motion, the propagation in cartesian coordinates and the conversion to Keplerian elements, is around 2,75 seconds.

The gaussian propagation involves the integration of another set of ordinary differential equations in the same time span as the cartesian propagation one. The equation of motion function though has in input the initial state in Keplerian elements, converts those in order to have a state vector and computes the J2 and SRP accelerations in {x,y,z} reference frame. Then the reference frame is changed in the {t,n,h} reference frame. After all, the function provides the derivatives on time of the Keplerian elements in the tangential – normal – out of plane reference frame. Finally, the integration is performed and we get the Keplerian elements at each time. As a way to do that, the computational time is about 2,17 seconds.

## 2.5 EVOLUTION OF THE ORBIT

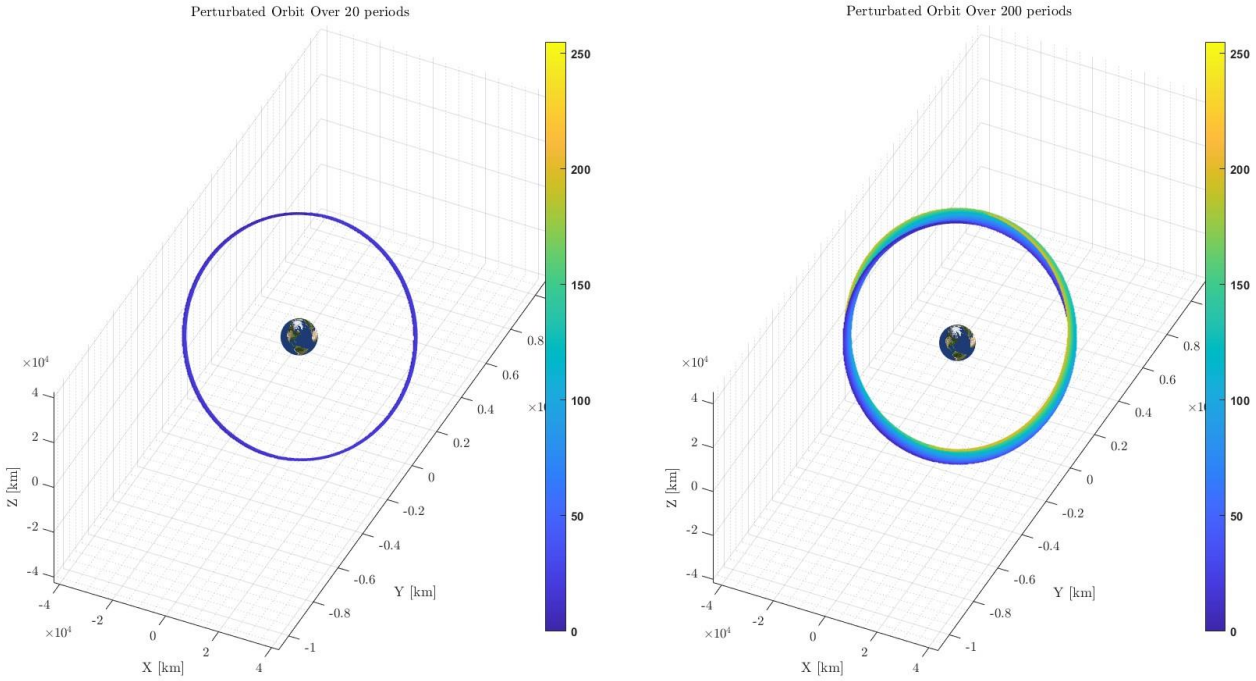


## 2.6 FILTERS

The team studied the orbital elements also using a low-pass filter in order to have a better understanding of the evolution of these. It removed all the high frequencies and gave back the secular evolution of each orbital element.
Nearly the initial and final borders we have two discontinuities, that can create some problems to the computation and the correct representation of the evolution of the Keplerian elements in these areas. Indeed, here the Gibbs phenomenon appears, but it is corrected considering the mean value of the secular evolution of the Keplerian elements just about the initial and final discontinuity.
We can here observe how the semi-major axis of the orbit, without considering the high frequencies, is absolutely constant. The secular evolution does not take in account any high oscillation around the mean value, so the filtered version is the constant initial value.

The eccentricity tends to increase without an oscillating behavior, thanks to the low-pass filter, and acts properly considering the solar radiation pressure, that increases the eccentricity of the orbit.
The inclination, considering the secular evolution, follows the bigger oscillation, and the perturbation is controlled in a span of 0,02°, nearly the 54° of inclination.
The right ascension of the ascending node doesn't oscillate anymore around the average value and tends to decrease accordingly to the secular evolution of Ω. The Nodal regression here is constantly decreasing.
The argument of pericentre increases due to the Perigee precession, caused by the J2 perturbation, but does not oscillate around the mean value, it is constantly increasing.
The true anomaly increases while the orbit is swept from 0° to 360°, and it is filtered using the low-pass filter.

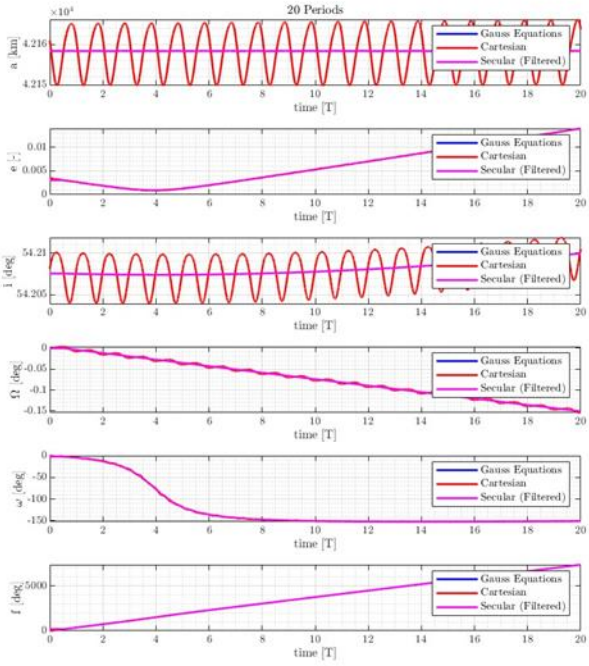


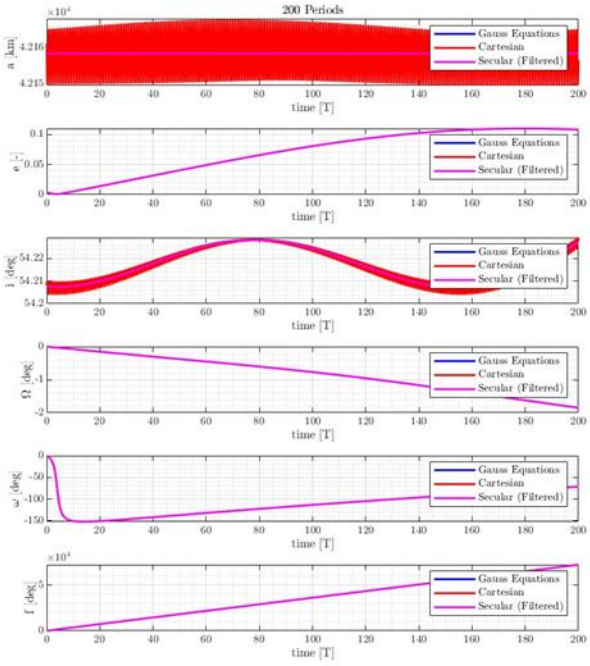


## 2.7 COMPARISON WITH REAL DATA

The team eventually performed a test for the propagation model that was created and used for the study. We downloaded the orbital elements of a satellite that has a similar orbit to the one assigned by the mission. The examined satellite is the ANIK C3, a Canadian geostationary communication satellite used for the TV broadcasting. We can now analyse the evolution of the real orbital elements and the propagated ones.
The real semi-major axis oscillates around the geostationary mean value with a period of about 65 orbital periods, while the propagated semi-major axis oscillates around the real value considering a span of ±10 kilometres. The error here stays in the order of $10^{-5}$, and oscillates considering the two armonic sequencies.
Considering now the eccentricity, we can observe that the real one remains constant while the perturbated one increases. That is due to the lack of control in the attitude dynamics of the perturbed propagation. Indeed, the real eccentricity is constant thanks to the control actions of

the satellite, that maintains the orbital elements in order to stay in the wanted orbit. The error here just increases because of that.
The inclination has the same evolution in both cases, and here increases until the 100 periods and will then decrease until the minimum describing an oscillatory evolution. The propagated evolution though has a lower oscillatory evolution, even having the same mean value, and that cause an increasing of the error near the maximum and minimum values of the harmonics.
The right ascension of the ascending node decreases in the considered cases due to the Nodal regression, but the real evolution decreases less thanks to the control system. For this reason, the error starts increasing from the beginning and continues with this behaviour.
The argument of perigee is different, looking to the two evolutions. The propagated one, accordingly to the theory, increases because of the Perigee precession, having an inclination lower than 63,4°. The real evolution instead has an oscillatory behaviour, which is conserved due to the control of the attitude dynamics. So here we have a curious trend of the relative error, which decreases until the evolutions are almost similar and the increases right after this moment.
The true anomaly, considering the two cases, increases from 0° to 360°, and the error is close to a constant value of $10^{-4}$, but at the beginning it is higher due to the discontinuity, and in the middle, due to the oscillation of the two armonics, it decreases until a minimum value of $10^{-7}$.